All-UV-written integrated planar Bragg gratings and channel waveguides through single-step direct grating writing

G. D. Emmerson, C. B. E. Gawith, S. P. Watts, R. B. Williams, and P. G. R. Smith

Optoelectronics Research Centre, University of Southampton, Southampton, SO17 1BJ, UK

Email: gde@orc.soton.ac.uk

S. G. McMeekin, J. R. Bonar, and R. I. Laming

Alcatel Optronics UK, Starlaw Park, Livingston, EH54 8SF

Abstract: We present a single-step technique for defining 2-dimensional integrated channel waveguide structures with internal Bragg gratings in photosensitive germanosilica-on-silicon substrates using two interfering focussed UV beams. Detailed device analysis of the relationship between the photosensitive properties of the glass, UV writing conditions, and subsequent refractive index change and channel waveguide strength is presented based on grating characterisation. Through software control, 300nm wide grating detuning across the E, S, C, L, and U wavelength bands is demonstrated.

Introduction: Direct UV writing [1-4] is a dynamic planar lightwave circuit fabrication technique offering great potential in the concept of rapid prototyping and small to medium lot batch fabrication. Based on a localized change in refractive index induced by short-wavelength radiation [5], this technique allows waveguide structures to be literally drawn into a photosensitive material by computer-controlled scanning of a focused UV beam, eliminating the development time and costs associated with repeated photolithographic steps. Each production run can be individually designed and tailored to the photosensitive properties of a particular material, allowing a wide range of devices to be written in a matter of hours. This process has previously been shown to be a versatile system producing high quality, low loss planar waveguide devices with a good compatibility to existing silica based telecom fibers [1].

A versatile technique combining closely packed channel waveguides with a Bragg grating tailored spectral response would allow the creation of compact systems for wavelength division multiplexing on a single optical chip. To achieve this goal the optimized integration of direct-UV-written waveguides and Bragg gratings within a planar geometry is of great significance, but to date the development of direct-UV-written channels with Bragg gratings have been limited to two-step fabrication process involving phase masks [2,6]. In such cases a primary exposure is often used to create a channel waveguide in the photosensitive material, while a secondary exposure is used to superimpose a grating structure. As the initial channel writing process often saturates the photosensitive response of the material, such sequential processes cannot be used to optimize both the grating strength and waveguide geometry in a single fabrication run.

To this end, we recently presented the first demonstration of simultaneously defined channel waveguides with integral Bragg gratings based on a small-spot interference pattern generated by two focussed UV-writing beams [7]. This single-step approach was developed to promote optimal use of sample photosensitivity for both the waveguide geometry and Bragg grating superstructure, with the potential for implementing many aspects of advanced grating design, such as chirp and apodisation, without the need for a phase mask. In this paper we present the results of several experiments to be derived from this direct grating writing process, including the characterisation of photosensitive material characteristics, single-step incorporation of planar Bragg gratings into two dimensional channel waveguide structures, and an unprecedented 300-nm-wide grating detuning response achieved across the E, S, C, L, and U wavelength bands, a technique controlled entirely through computer software and requiring no modifications to our experimental setup.

Direct grating writing: In our direct grating writing arrangement, two UV-writing beams are individually focused and aligned to create a single writing spot with an intrinsic interference pattern defined by the wavelength and intersection angle of the beams (Figure 1). As the sample is translated relative to the spot, the intensity of the laser is modulated with a period such that the maxima of the intensity pattern in the writing spot overlaps the maxima of the previous exposure, inducing a channel waveguide with an inherent Bragg grating index modulation. When the sample is translated under a constant writing beam, the intra-spot interference pattern is averaged out and the focussed spot can be used to write standard channel waveguide structures, including the curves and junctions that form the basic building blocks of larger integrated optical systems. The combination of these two techniques allows planar Bragg gratings to be inserted into complex UV-written devices in a single processing step, and is achievable as a direct result of the small writing spot fundamental to these processes.

One of the most significant advantages of this direct grating writing technique is that the required characteristics for both the planar Bragg grating and channel waveguide structures are predetermined entirely under computer control, and are thus not dependent on any time consuming changes to the physical setup. Using this technique we have demonstrated a system of unparalleled flexibility in the center wavelength detuning range of planar Bragg gratings that can be achieved in a single fabrication step, with no alteration to the optical alignment or components.

Center-wavelength detuning: To date, the majority of planar Bragg grating fabrication techniques still use a phase mask in stationary contact, or near contact, with a photosensitive substrate such that the relative position of the interference pattern is fixed to a single alignment on the sample [2,6]. The phase mask is a very accurate and controllable method for defining the interference pattern period, also allowing for sophisticated grating structures set at the mask design stage. However, whilst this stationary method can produce very good grating profiles, a phase mask can only produce a single fixed grating structure.

In fiber Bragg grating production the flexibility of the grating writing was significantly enhanced by moving the fiber relative to the interference pattern [8]. This technique builds up the grating by overlapping successive exposures, with each exposure making up only a small part of the resultant structure but being displaced by an integer number of grating periods. Thus, gratings can be written that are longer than the incident interference pattern, resulting in the decoupling of the resulting Bragg grating structure from the original interference pattern used to inscribe the structure.

A significant advantage to arise from the decoupling of the grating structure from the interference pattern is that of center-wavelength detuning, a process where the distance between exposures is an integer number of grating planes plus an offset Δ. The result of the offset Δ over the multiple exposures is an index modulation with a period of $(\Lambda + \Delta)$, where Λ is the period of the interference pattern. This detuning process allows a range of grating periods to be achieved from a single interference pattern, reducing the cost of fiber Bragg grating production systems by allowing a single 'good quality' phase mask (or region of a phase mask) to produce a variety of Bragg grating periods or chirped structures, but at the same time reduces the contrast of the grating. The resultant contrast is dependent on the magnitude of the detuning parameter and the size of the writing spot, such that the contrast can range from maximum when $\Delta = 0$ and the overlapping is constructive, to minimum contrast when the first and last grating plane from exposures that overlap are π out phase. The point of minimum contrast can be expressed as $\Delta = \pm(\Lambda/N)$, where N is the width of the spot in periods of the interference pattern.

For the work described in this paper, it is important to note that the maximum attainable detuning range is inversely proportional to the width of the interference pattern. This is significant as the writing spot used in our direct grating writing process is based on an envelope diameter of 4μm with a 532nm interference pattern period, resulting in only 8 interference fringes being written during each individual exposure. Compared to phase-mask-based schemes, where typical envelope sizes of >100μm limit detuning to the order of around ±20nm, the extremely small writing spot used in our process allows a much greater range of detuning from the native interference pattern than has traditionally been possible. Thus we are able to define a wide range of grating structures using only a single fixed interference pattern.

Experimental: Fabrication of the direct-written gratings described in this paper was performed using a frequency-doubled 244nm argon-ion laser, a high precision 3-dimensional translation stage, and an interferometrically controlled acousto-optic modulator. A beam splitter was used to create two separate beam paths at an intersection angle of 29 degrees, and both beams were individually focused and aligned to give a single 4μm interfering spot. Each device was fabricated in three layer silicon-on-silica substrates provided by Alcatel Optronics UK, where the core layer was co-doped with germanium to produce an intrinsic photosensitivity that was subsequently enhanced through hydrogen loading at 150bar for 1 week. For these experiments a range of planar Bragg gratings based on variations of period, length, channel waveguide structure, and UV-writing conditions (speed, power, etc.) were written.

After the UV writing process each sample was left to out-diffuse any remaining hydrogen before analysis. The Bragg grating structures written for sample analysis and 2-dimensional integration were analyzed using an EDFA-based fiber-coupled ASE source. For the wide wavelength detuning experiment a fiber-coupled white light source was used to give an extended range of measurement. In each case the fiber launch into the channel was aided through index matching fluid, and the transmitted spectra was recorded on an optical spectrum analyzer. Reflected spectra were recorded by utilizing a 3dB coupler on the launch fiber to access the reflected signal.

Results and discussion: As direct grating writing defines both a channel waveguide and Bragg grating simultaneously, with the only difference between the fabrication of separate channel waveguide and Bragg grating sections being the on/off modulation of the laser, the power and writing conditions can be very closely matched for both structures. Thus, by interrogating the response of the grating section, accurate information about both the channel waveguide and Bragg structures can be obtained. For example, Figure 2 shows a typical reflection spectra from a channel waveguide with 10mm long integral Bragg grating section, where a grating period of 532nm gives a peak reflection at 1542.8nm and a bandwidth of 0.216nm. Using the Bragg relation ($\lambda_b = 2\Lambda n_{eff}$, where λ_b is the peak reflected wavelength, Λ is the grating period, and n_{eff} is the effective refractive index of the waveguide) and accurate knowledge of the grating period such measurements offer an ideal method of accurately and efficiently determining the effective index of a guided mode in the waveguide, and hence the strength of the UV induced channel index.

From these experiments we have found that the UV-induced refractive index change of the material and its relationship with the writing beam power depends greatly on the processing history of the sample. Using the convention typically applied in direct UV writing the writing conditions have been expressed in terms of fluence (Equation 1)[1]:

$$F = \frac{I_{UV} \times a}{v_{scan}} \qquad (1)$$

where F is the fluence (KJcm^{-2}), I_{UV} is the average power density in the writing spot (KJcm^{-2}s^{-1}), a is the writing spot diameter (cm) and v_{scan} is the translation velocity (cms^{-1}). Fluence is an expression of the energy exposed to the material in the writing process and is a common parameter used to describe direct UV writing.

The graph presented in Figure 3 provides a plot of effective refractive index in a channel waveguide against UV writing fluence, with data further categorized based on the power of the writing spot. From this measurement is clear that fluence alone does not provide an accurate means of describing refractive index change during the UV writing process. Instead it should be noted that, counter-intuitively, the strength of the channel waveguide increases as the writing power is reduced for exposures of the same fluence (corresponding to a slower translation velocity). This effect is consistent throughout the range of fluences used, becoming more pronounced in the low fluence regime. From the graph it is apparent that this hydrogen-loaded sample exhibits a distinct threshold effect at fluences of $10KJcm^{-2}$, below which channel waveguides are no longer created. The exact point where this threshold occurs varies with the power of the writing beam, again with slower translation speeds crossing the threshold effect at lower fluences.

Further information about the UV-written waveguide can be obtained via a comparison of the position of the reflected wavelength peaks in spectra from TE or TM polarized light, giving a typical birefringence of $3.3x10^{-4}$ in these samples. A typical mode profile from a channel waveguide with a 10mm long integral Bragg grating section is also presented in Figure 4, from which far-field imaging of the guided mode can be used to provide a value for the refractive index change in the sample, yielding an approximate NA of 0.12±0.2.

In order to demonstrate the 2D capabilities of our direct grating writing technique, Mach-Zender structures were written in a single-step based on the arrangement illustrated in Figure 1. For each device two 5mm-long cosine-style y-splitter sections were used to separate the two central arms of the structure by 200μm, corresponding to s-bend radii of ~ 60mm. For these initial experiments two 8mm long planar Bragg gratings with periods of 532 and 532.4nm respectively were incorporated into the two arms of each device, resulting in dual-peak spectral responses typical of that given in Figure 5. From the graph the distinction between the two grating reflection responses is clear, and future work will be aimed at integrating such gratings into larger optical systems.

The center-wavelength detuning range attainable using our small-spot interference pattern was demonstrated by producing a wide array of grating periods. From the single fixed experimental setup, a range of grating periods from 480nm to 580nm were produced, all controlled by varying the distance translated between subsequent exposures. The period of each grating structure was defined through software control with the intersection angle of the two writing beams remaining constant throughout the entire experiment. The structures defined in this experiment each included a 10mm long grating section with lead-in and lead-out channel waveguides written using the same fluence as in the grating section. It is again noted that our extremely small writing spot allows a much greater range of detuning from the native interference pattern than has traditionally been possible. This effect is dramatically demonstrated in the graph of Figure 6, where an effective detuning range of ~300nm, across the E, S, C, L, and U wavelength bands, is presented.

Conclusions: In conclusion, we present a direct grating writing technique that allows simultaneous UV definition of channel waveguides with integral Bragg gratings in a photosensitive planar media. Based on a small-spot interference pattern generated by two focused UV-writing beams, this single-step approach was developed to promote optimal use of sample photosensitivity for both the waveguide geometry and Bragg grating superstructure, with the potential for implementing many aspects of advanced grating design, such as chirp and apodisation, without the need for a phase mask. Early results based on detailed grating characterization and analysis of the photosensitive properties of the glass, UV writing conditions, and subsequent refractive index change and channel waveguide strength have been presented and provide potential application for a rapid route towards optimized compositions in photosensitive substrates.

By combining the process of direct grating writing and center wavelength detuning we have demonstrated a range of Bragg gratings with spectral responses that cover the E, S, C, L, and U wavelength bands, with the structure of both the waveguide and gratings defined entirely in software. The inherent flexibility of our small interference spot based system allows the formation of virtually any grating period required in the standard or extended erbium compatible bands in a single fabrication step-up, while also allowing single-step incorporation of planar Bragg gratings into two-dimensional structures. As the entire direct grating writing process is performed without the use of a phase mask, each device or production run on the system can be individually tailored to suit the photosensitive properties of the host material, without any need to change the experimental set-up or alignment.

Future work based on these encouraging results will focus on the use of direct grating writing as a means towards optimizing photosensitive material compositions and creating compact systems for wavelength division multiplexing on a single optical chip.

References:

[1] M. Svalgaard and M. Kristensen, "Directly UV-written silica-on-silica planar waveguides with low loss" Electron. Lett. **33**, (10), 861-863 (1997)

[2] M. Svalgaard, "Optical waveguides and grating made by UV-photogeneration" ECIO, Turin, Italy, 333-338 (1999)

[3] C. B. E. Gawith, A. Fu, T. Bhutta, P. Hua, J. Wang, E. B. M. Taylor, D. P. Shepherd, P. G. R. Smith, D. Milanese, and M. Ferraris, "Direct-UV-written single-mode buried laser channel waveguides in direct-bonded intersubstrate ion-exchanged neodymium-doped germano-borosilicate glass", Appl. Phys. Lett. **81**, (19), 3522-3524 (2002)

[4] J. –S. Koo, R. B. Williams, C. B. E. Gawith, S. P. Watts, G. D. Emmerson, V. Albanis, P. G. R. Smith, and M. C. Grossel "UV written waveguide devices using crosslinkable PMMA-based copolymers" Electron. Lett. **39**, (4), 394-395 (2003)

[5] K. O. Hill, Y. Fujii, D. C. Johnson, and B. S. Kawasaki, "Photosensitivity in optical waveguides: Application to reflection filter fabrication", Appl. Phys. Lett. **32**, (10), 647-649 (1978).

[6] M. Y. Park, W. Yoon, S. Han, and G. H. Song, "Fabrication of low-cost planar wavelength-selective optical add-drop multiplexer by employing UV photosensitivity" Electron. Lett. **38**, (24), 1532-1533 (2002)

[7] G. D. Emmerson, S. P. Watts, C. B. E. Gawith, V. Albanis, M. Ibsen, R. B. Williams and P. G. R. Smith, "Fabrication of directly UV written channel waveguides with simultaneously defined integral gratings" Electron. Lett. **38**, (24), 1531-1532 (2002)

[8] M. J. Cole, W. H. Loh, R. I. Laming, M. N. Zervas and S. Barcelos, "Moving fibre/phase mask-scanning beam technique for enhanced flexibility in producing fiber gratings with uniform phase mask", Electron. Lett. **31**, (17), 1488-1490 (1995)

Figure captions:

Figure 1: Single-step direct grating writing of integrated channel waveguides and Bragg grating structures.

Figure 2: Reflection spectra of a 10mm long Bragg grating with a bandwidth of 0.216nm.

Figure 3: A graph of effective refractive index versus fluence for a range of peak writing beam intensities in a hydrogen loaded silica-on-silicon sample.

Figure 4: Mode profile of a channel waveguide and Bragg grating structure at a wavelength of 1.55μm.

Figure 5: Dual-peak reflection spectra for a 2-dimensional Mach-Zender channel waveguide structure incorporating two Bragg gratings of different periods.

Figure 6: Demonstration of center-wavelength detuning applied to direct grating writing. Bragg gratings with wavelength responses across the E, S, C, L, and U bands are presented.

Figure 1:

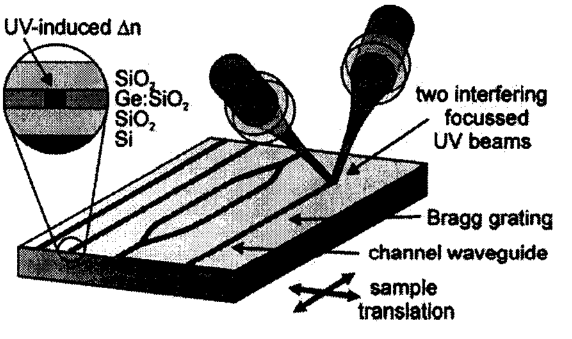
UV-induced Δn
SiO2
Ge:SiO2
SiO2
Si
two interfering
focussed
UV beams
Bragg grating
channel waveguide
sample
translation

Figure 2:

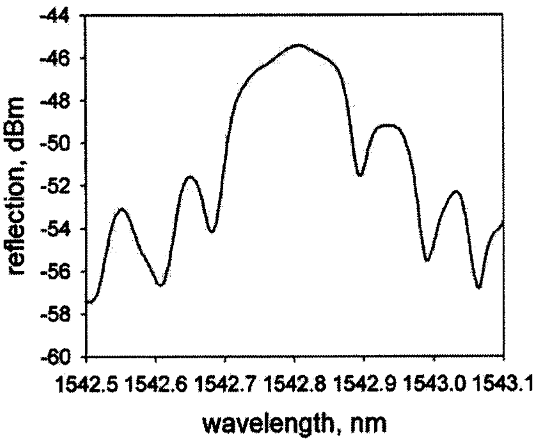

-44
-46
-48
-50
-52
-54
-56
-58
-60
reflection, dBm
1542.5 1542.6 1542.7 1542.8 1542.9 1543.0 1543.1
wavelength, nm

Figure 3:

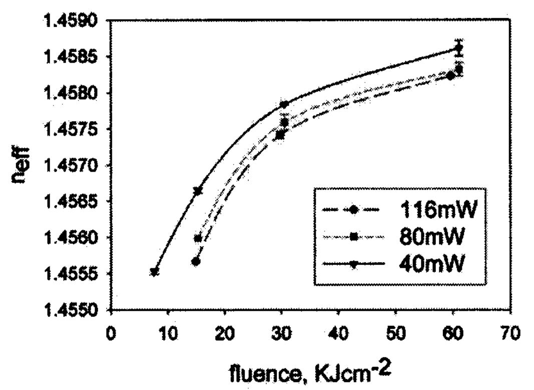

1.4590
1.4585
1.4580
1.4575
1.4570
1.4565
1.4560
1.4555
1.4550
neff
0
10
20
30
40
50
60
70
fluence, KJcm-2
116mW
80mW
40mW

Figure 4:

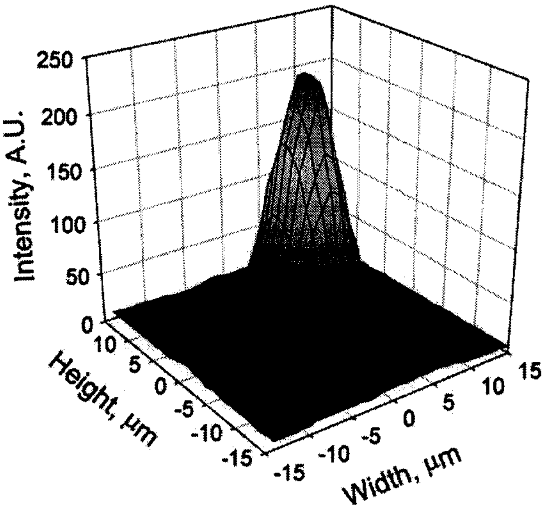

250
200
150
100
50
0
Intensity, A.U.
10
5
0
-5
-10
-15
Height, µm
-15
-10
-5
0
5
10
15
Width, µm

Figure 5:

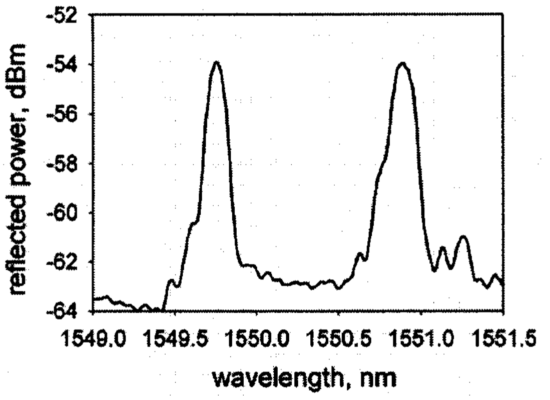

-52
-54
-56
-58
-60
-62
-64
reflected power, dBm
1549.0 1549.5 1550.0 1550.5 1551.0 1551.5
wavelength, nm

Figure 6:

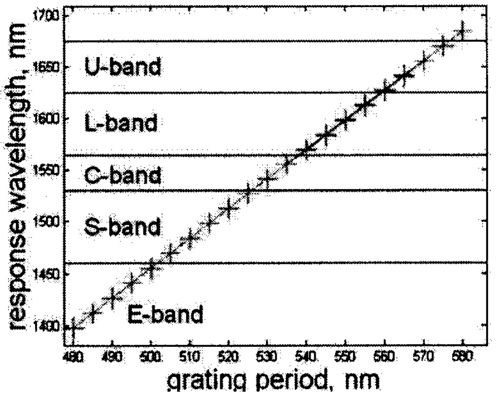

U-band
L-band
C-band
S-band
E-band
response wavelength, nm
grating period, nm
1700
1650
1600
1550
1500
1450
1400
480
490
500
510
520
530
540
550
560
570
580